Study of Cu diffusion in Be using ion backscattering*

S. M. Myers, S. T. Picraux, and T. S. Prevender
Sandia Laboratories, Albuquerque, New Mexico 87115
(Received 28 September 1973)

The diffusion of Cu in single-crystal Be has been studied as a function of temperature, crystal orientation, and method of Cu introduction. Concentration-versus-depth profiles were obtained from the energy spectra of backscattered 2-MeV He^+ and 2-MeV protons. The Cu was introduced by ion implantation at 100 keV or by vapor deposition. Reliable values of the dilute diffusion coefficient D were obtained from the implanted samples when the Cu had diffused more than a factor of 2 beyond the initial implanted range ($\simeq$900 Å), whereas anomalous diffusion rates were found over shorter distances. The vapor-deposited Cu films were not used to determine D values, primarily because of substantial surface oxidation. However, the qualitative behavior of the three-component system Be-Cu-O was interpreted in terms of intermetallic compound formation and the heats of formation of the respective metal oxides. For example, whenever Be and Cu are present together, gettering of oxygen by Be is observed, and a surface layer of BeO is formed from which Cu is excluded. Also, the solubility of Cu in hcp Be at 750 °C was measured to be 5.5 ± 1.0 at.%, in good agreement with the published phase diagram. The coefficient D was measured for Cu diffusion along both the c and a crystallographic axes of the hcp Be lattice, between 420 and 640 °C. There is a significant anisotropy, with $D_c/D_a = 0.5 \pm 0.1$ at 600 °C. These results merge smoothly with those obtained by Dupouy, Mathie, and Adda over the range 700–1000 °C, by the radioactive-tracer method. The combined data represent a variation in D of a factor of $\simeq 5 \times 10^6$ and permit an accurate determination of the activation energies. These are 2.00 ± 0.10 eV for the a axis and 2.05 ± 0.10 eV for the c axis. The LeClaire theory of heterovalent impurity diffusion was used to compare the Cu results with Be self-diffusion data of Dupouy, Mathie, and Adda. This theory was found to be inconsistent with the observed overall difference in activation energies between Cu and self-diffusion, and also with the observed anisotropy for Cu diffusion. In order to determine the sensitivity of the diffusion rate to radiation damage, a sample was bombarded with a flux of $\simeq 3 \times 10^{13}$ Ne^+/cm^2 sec during a 30-min anneal at 500 °C. The resulting rate of atomic displacement, $\simeq$0.01 dpa/sec for depths $<$5000 Å, was not sufficient to produce an observable change in the diffusion rate.

I. INTRODUCTION

The diffusion of Cu in single-crystal Be has been studied using ion backscattering to determine the Cu concentration versus depth. Preliminary results for implanted Cu were given previously.[1] Here detailed findings are reported for Cu introduction by ion implanation and also by thin-film deposition. Diffusion measurements by others have employed the radioactive tracer method, and have been made for temperatures above 700 °C.[2] The present results provide not only a comparison between complementary experimental techniques, but also extend to considerably lower temperatures the range over which the diffusion coefficient D is known. In addition, we have examined in some detail both the anneal behavior of Cu films on Be and effects unique to Cu implantation.

The coefficient D for dilute Cu in Be is also of theoretical interest. Be has the hcp crystal structure, with the smallest value of c/a of all the hexagonal metals, 1.567. This means that nearest neighbors in adjacent basal planes are closer than those in the same basal planes by a factor of 0.973. One consequence of the noncubic symmetry is that the diffusion rate is expected in general to vary with direction. This anisotropy permits a doubly sensitive test of any proposed theoretical picture, because it increases the observable information to be accounted for without expanding the list of input parameters. The particular case of group I B impurities in Be warrants special attention because Cu and Ag, both in this group, have been reported to behave quite differently. For example, at 700 °C one has $D_c/D_a = 0.5$ for Cu in Be[2] and $D_c/D_a = 1.8$ for Ag in Be.[3] Furthermore, by combining the heterovalent diffusion theory of LeClaire[4] with measured Be self-diffusion results,[5] as will be discussed below, one predicts $D_c/D_a = 0.13$. This differs strongly from the experimental ratios, especially that for Ag in Be.

The ion-backscattering technique has been widely employed recently in the study of near-surface phenomena.[6] In several cases it has been applied to intermetallic diffusion.[7–11] In Be, the depth resolution is ~ 0.03 μm to a total depth of ~ 2 μm using 2-MeV He^+ and is ~ 0.3 μm to a depth of ~ 10 μm using 2-MeV protons. This relatively high resolution combined with a nondestructive character allows comparative measurements as a function of time and temperature on the sample, and makes the technique suitable for measuring small diffusion constants. It is also a convenient probe for examining in detail the frequently encountered

problem of surface trapping of the impurity. Limitations are an inability to distinguish between elements of similar mass, and a low sensitivity to light impurities in heavy hosts. Maximum sensitivity is achieved for a heavy impurity contained in a light host, a situation realized for the present studies of Cu in Be.

In most cases we have used ion implantation to introduce Cu directly into the Be host, with a resulting local concentration peak of 4–8 at.%. In this way we have avoided the problem of near-surface trapping of the impurity which often arises when surface deposition is used. Such trapping may result, for example, from a surface oxide on the host, oxidation of the impurity layer during annealing, or intermetallic compound formation. It is especially important that such effects be absent when the diffusion distances of interest are as small as those measured by ion backscattering. In some cases, however, the diffusant may be tied up even when implanted. Implantation has previously been used to introduce the diffusants Fe, Mn, In, and Zn into Al[10,12–14]; and for Fe and Zn significant trapping was reported. In the case of Zn a careful study of the problem indicated that Al_2O_3 was being formed to a depth sufficient to encompass the implanted atoms.[10] Work presently underway on Au in Be[15] and Sb in Al[16] indicates that when the implanted concentration is significantly above the solubility limit, normal thermal diffusion is inhibited. Such behavior, for example, can be due to precipitation or to damage trapping. Thus implantation does not necessarily produce simple source boundary conditions for the diffusion equation, and consequently each case must be considered individually. In the present work the implanted Cu concentrations were of the order of the solubility limit for Cu in Be. The implantation proved quite successful in avoiding the trapping problem and at no time was an anomalous surface peak observed in the diffusion profiles.

Measurements were made on Be samples which had been vapor deposited with Cu in order to (i) compare with the implant results and thereby assess the relative merits of the two methods; (ii) extend the data to higher temperatures, where practical numbers of implanted Cu atoms were insufficient to permit accurate determination of D; and (iii) study the Be-Cu system at higher Cu concentrations. As will be discussed, oxidation of the Cu layer during annealing and formation of Be-Cu intermetallic compounds prevented the extraction of accurate dilute diffusion coefficients. However, the qualitative features of the film behavior during annealing could be accounted for in a straightforward manner, and these resulted in several general conclusions concerning the Be-Cu-O system.

In Sec. II the diffusion equation is reviewed as it applies to the present experiment, and the LeClaire theory is applied to predict the activation energies. Experimental procedures are described in Sec. III, and the results and analysis are presented in Sec. IV.

II. THEORY

A. Diffusion equation

The equations governing diffusion in the dilute limit, in the presence of a plane at position $x=0$ through which there is no net flow of Cu atoms, are

$$D\frac{d^2}{dx^2}C(x,t)=\frac{d}{dt}C(x,t) \tag{1}$$

and

$$\lim_{x\to 0}\left(\frac{d}{dx}C(x,t)\right)=0, \tag{2}$$

where C is the Cu concentration and t is the time. The general solution for this case is given by[17]

$$C(x,t)=[2(\pi Dt)^{1/2}]^{-1}\int_0^\infty C_0(y) \times(e^{-(y-x)^2/4Dt}+e^{-(y+x)^2/4Dt})\,dy\,, \tag{3}$$

where $C_0(x)=C(x,0)$ is the Cu initial profile. For the purposes of the present work it will be shown that accurate values of D can be obtained from measurements of the profile width when the initial profile is approximated by

$$C_0(x)=K(\pi Dt_0)^{-1/2}e^{-x^2/4Dt_0}\,, \tag{4}$$

where K and t_0 are adjustable constants. Then Eq. (3) reduces to

$$C(x,t)=K[\pi D(t+t_0)]^{-1/2}e^{-x^2/4D(t+t_0)}\,. \tag{5}$$

Defining the profile width $W(t)$ such that

$$C(W,t)=\tfrac{1}{2}C(0,t)\,, \tag{6}$$

one has from Eq. (5)

$$[W(t)]^2=4Dt\ln(2)+[W(0)]^2\,. \tag{7}$$

Thus the slope of a plot of $[W(t)]^2$ vs t yields the diffusion coefficient D. This was our standard mode of analysis for obtaining D, and was used except for two anneal sequences where an analytic fit was made to $C_0(x)$ and Eq. (3) was applied. By adjusting the value of D for a best fit to measured isothermal profiles, consistency with the simplified analysis of Eq. (7) was demonstrated.

Two features of the solution of Eqs. (1) and (2) allow a sensitive check on whether these equations correctly describe the diffusion. First, from the general solution Eq. (3), the concentration profile should approach a Gaussian shape as annealing proceeds. If it starts as a Gaussian, then it

should remain so. By using the analytic fit to $C_0(x)$ together with Eq. (3) to calculate the profile it is possible to directly check that the shape of the diffused profiles are in agreement with prediction. Second, after a Gaussian shape is reached, $[W(t)]^2 \propto t$. If, for example, the diffusion coefficient D were concentration dependent in the concentration range of the experiment, or if near-surface trapping of the Cu were present, these conditions would not be met.

B. Anisotropy

As mentioned previously, the absence of cubic symmetry in the hcp structure permits anisotropy of the diffusion rate. The analysis of this problem has been described in some detail,[18,19] and here we simply outline the features relative to the present work. There are two inequivalent jumps between near-neighbor lattice sites, one within the same basal plane (perpendicular to the C axis) and one to an adjacent basal plane. The former we label α, the latter β, with the associated characteristic jump rates being τ_α^{-1} and τ_β^{-1}. The diffusion rates along the A and C crystalline axes are then given by

$$D_A = \tfrac{3}{2}a^2 f_{\alpha A}\tau_\alpha^{-1} + \tfrac{1}{2}a^2 f_{\beta A}\tau_\beta^{-1} \tag{8}$$

and

$$D_C = \tfrac{3}{4}c^2 f_{\beta C}\tau_\beta^{-1} , \tag{9}$$

where a and c are the crystalline lattice parameters. The correlation factors f take account of the presence of the vacancy left behind the jumping atom, which makes a reversing jump more probable than other jumps. By definition, $0 < f < 1$. The exact values depend in a complicated way on τ_α^{-1} and τ_β^{-1}, and also on the host atom jump rates. In general they are temperature dependent.

For Cu diffusion in Be over the temperature range of the experiment, τ_α^{-1} and τ_β^{-1} are smaller than the host-atom jump rates by a factor of order 10^{-2}. It may be argued qualitatively that under these conditions all of the correlation factors are very nearly unity, since the vacancy left in the wake of the impurity will be fully randomized before a reversing jump can occur. This is readily confirmed by applying the equations for f given in Ref. 19. For Be self-diffusion the factors f differ substantially from unity, and cannot be neglected. However, their temperature dependence is small in comparison to that of the factor τ^{-1}.

C. LeClaire theory

In this paper we shall use the LeClaire theory[4,19] to relate the activation energies for diffusion of Cu in Be to those for Be self-diffusion. This approach has met with some success, for example, with group-IB hosts containing impurities to the right of the IB column in the Periodic Table.[18] However, it has proved less satisfactory in certain other cases, such as impurity diffusion in Al.[20] The weakness seems to lie in the assumed effective impurity-vacancy potential, which is not generally realistic. However, in the current absence of a better theory for diffusion in Be, we proceed while keeping in mind the problems.

In the LeClaire model, a substitutional impurity is assumed to differ from a host atom only in that its valence Z_i is different from the host valence Z_h. A vacancy which moves into the vicinity of the impurity will be subjected to a change in electrostatic potential ΔV which is proportional to $(Z_i - Z_h)$. The form of this potential is taken to be

$$\Delta V(r) = \gamma(e/r)(Z_i - Z_h)\, e^{-qr} , \tag{10}$$

where

$$q^2 = (4me^2/\hbar)(3n_0/\pi)^{1/3} , \tag{11}$$

m is the electron mass, e is its charge, n_0 is the number density of conduction electrons, and γ is a dimensionless factor of order 1. The exponential factor results from the Thomas-Fermi screening by the conduction electrons. The vacancy is assumed to have an effective charge of $-Z_h e$, so that the energy of interaction is $-Z_h e \Delta V(r)$.

To evaluate the difference in activation energy ΔQ from that of self-diffusion, the impurity is considered to be located at the saddle point between the two lattice sites involved in the jump of interest. It is then flanked by two half-vacancies, whose charges are assumed to be located at the centroids of the respective hemispheres. Then

$$\Delta Q = -Z_h e \Delta V(r = \tfrac{11}{16}\lambda) , \tag{12}$$

where λ is the distance between the two lattice sites. This activation energy is for the impurity jump rates τ^{-1} of Eqs. (8) and (9), and hence does not involve the temperature dependence of the correlation factors f. Applying this result to the diffusion of Cu in Be, for which $Z_i = 1$, $Z_h = 2$, $\lambda_\alpha = 2.287$ Å and $\lambda_\beta = 2.225$ Å, we obtain $\Delta Q_\alpha = +0.80$ eV and $\Delta Q_\beta = +0.90$ eV, respectively, for the two kinds of jump.

III. EXPERIMENTAL PROCEDURES

Beryllium single crystals approximately $10 \times 10 \times 3$ mm were obtained from the Franklin Institute. The large faces had been spark cut and then electropolished to remove the damage. X-ray measurements on one of the samples indicated a mosaic spread of $\simeq 0.6°$ full width at half-maximum (FWHM) over the 1-cm^2 face. This spread should have a negligible effect on the diffusion results, but it precluded lattice location of the Cu by the

channeling technique. The implantations were performed at room temperature using 100-keV Cu^+. During implantation the crystal faces, which had been cut perpendicular to either the c or a crystalline axis, were tilted 8° from the normal to the beam to avoid channeling effects. One sample was implanted to 7×10^{15} Cu/cm^2 at 0.3 μA/cm^2, the remainder to $(4-8)\times10^{16}$ Cu/cm^2 at $\simeq 1$ μA/cm^2. The Cu films, vapor deposited onto the Be under $< 5\times10^{-6}$ Torr background pressure, were brought to nominal thicknesses of either 300 or 3000 Å.

The backscattering measurements were made with 2-MeV He^+ and 2-MeV protons from a Van de Graaf accelerator. Particles backscattered at an angle of 170° were energy analyzed with a surface barrier Si detector whose resolution was $\simeq 13$ keV FWHM, corresponding to $\simeq 300$-Å depth resolution for α's and $\simeq 3000$ Å resolution for protons. Most of the anneals were done in a tubular furnace under flowing dry nitrogen. For some of the samples with vapor-deposited films, flowing forming gas (10-at.% H_2, 90-at.% N_2) was used. The sample was held on a movable quartz support, which had a Chromel-Alumel thermocouple junction in close proximity to the sample. Rapid thermal equilibration (usually within 20 °C of final temperature in less than 3 min) was achieved by inserting the holder after the furnace had been brought to temperature, and removing it to stop the anneal. The temperature of the furnace was regulated to better than ± 5 °C. We estimate that additional errors, from causes such as imperfections in the thermocouple wire and temperature differentials between sample and junction, add no more than ± 3 °C to the total uncertainty in the absolute temperature. The 260-keV Ne bombardment at 500 °C, as well as one 750 °C anneal sequence on a vapor-deposited sample, were performed at a pressure of $< 10^{-6}$ Torr. The uncertainties in temperature were ± 10 °C for the former, and ± 20 °C for the latter.

IV. RESULTS AND DISCUSSION

A. Implanted Cu

Two representative spectra for 2-MeV He^+ backscattered from Cu-implanted Be are shown in Fig. 1. The locations of the higher energy edges of the various peaks are determined by the recoil energy loss of the probe particle during the nuclear backscattering event: The lighter the target nucleus, the greater the energy loss. α particles scattered from nuclei beneath the surface suffer an additional energy loss to electronic excitations while passing through the solid. Hence the energy distribution of backscattered particles can be directly related to the concentration-versus-depth profile.[21] In the present experiment, the depth scale was obtained by performing a numerical integration of energy loss rate S over the particle path, using published experimental results for S in Be as a function of energy.[22] The effect of the implanted Cu on the energy loss rate was small in comparison to the experimental resolution, and was therefore neglected.

The as-implanted spectrum in Fig. 1 (solid line) shows the implanted Cu (4×10^{16} Cu/cm^2), a thin surface layer of BeO (6×10^{16} O/cm^2), and some surface C (5×10^{16}C/cm^2). The carbon is probably introduced by the breakdown of residual hydrocarbon gases by the implantation beam. The energy corresponding to Cu at the surface (arrow in Fig. 1) was determined from a separate backscattering

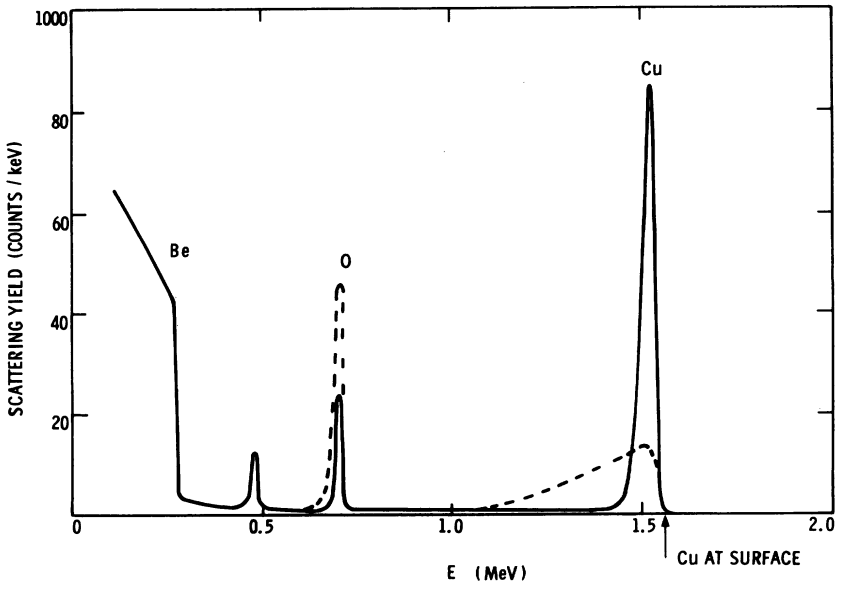

FIG. 1. Energy spectrum of 2-MeV He^+ backscattered at 170° from Cu implanted Be. Solid line: no anneal. Dashed line: after 36 min at 595 °C. Peak areas correspond to areal concentrations of 4×10^{-16} Cu/cm^2 for the implant, and surface impurities of 6×10^{16} O/cm^2 before annealing and 2×10^{17} O/cm^2 afterward, and 5×10^{16} C/cm^2.

profile taken on a Cu foil for the same incident energy. After a 36-min anneal at 595 °C the spectrum in Fig. 1 (dashed line) indicates that the Cu has diffused deeper into the Be host, with the half-amplitude concentration point falling at 5000 Å. There is also an increase in surface oxide during the anneal to 2×10^{17} O/cm^2. Close inspection of the Cu profile shows that it does not extend to the surface following the anneal. This is due to the presence of the BeO layer. Indeed, as will be discussed in Sec. IV B, we found that whenever a mixture of Cu and Be was oxidized, BeO formed and the Cu was excluded.

The as-implanted Cu profile deduced from the energy spectrum of Fig. 1 is shown in Fig. 2, along with that for the lowest-fluence implant. The similarity of the shapes would seem to rule out any strong dependence of the profile on flux and fluence for the range of values used. Both these profiles are for c-axis samples, but the a-axis results were the same to within the experimental uncertainty. This experimental distribution, with a peak position of (900 ± 100) Å and a width of (850 ± 100) Å FWHM, may be compared with predictions of the LSS theory.[23] Brice[24] has applied this theory to the case of 100-keV Cu in Be, and has obtained 680 Å for the projected range and (165 Å)^2 for the second moment about the projected range. The values of these theoretical parameters are different from those given in Ref. 1 because of an error in the previous calculation. The solid curve in Fig. 2 was constructed from these numbers by assuming a Gaussian shape, by adding the second moment of the detector resolution function to the theoretical second moment to take account of the associated broadening of the experimental profile, and by normalizing the peak amplitude to that of the data. There is fair agreement between theory and experiment. The peak in the experimental profile is shifted to greater depth by ≃200 Å. We note that any sputtering during implantation would increase this discrepancy. However, for these implantation fluences the correction is small. For example, using the sputtering ratio of 2.0 for 60-keV Kr incident on Be,[25] and assuming that approximately the same ratio holds for 100-keV Cu incident on Be, one estimates that ≃80 Å would be removed at the higher fluence of Fig. 2. There is also an extended tail toward greater depths in the experimental profile. Such tails have often been observed for implantation in Si.[26] The effect may be due to damage-enhanced diffusion during the room-temperature implantation, or to partial channeling of the Cu$^+$ beam.

In order to interpret the thermal diffusion of the Cu we begin with the general solution to the diffusion equation with boundary condition Eq. (2), as given by Eq. (3). The choice for the starting concentration profile $C_0(x)$ is represented by the dashed line in Fig. 2, and is the sum of two Gaussians with parameters adjusted to fit the data. The $x=0$ plane, i.e., the plane across which no net flow of Cu occurs, is located at a depth of ≃400 Å. This was done because of the formation upon heating of a layer of BeO from which the Cu was excluded. Thus the reflecting barrier for diffusion lies at the BeO-Be interface rather than the surface, and $x=0$ in the calculation has been chosen to correspond to the apparent edge of this interface barrier following annealing. The size of the shift is small compared to the thermal diffusion distances of interest, and therefore the details of the handling of this shift should not significantly alter the D values obtained.

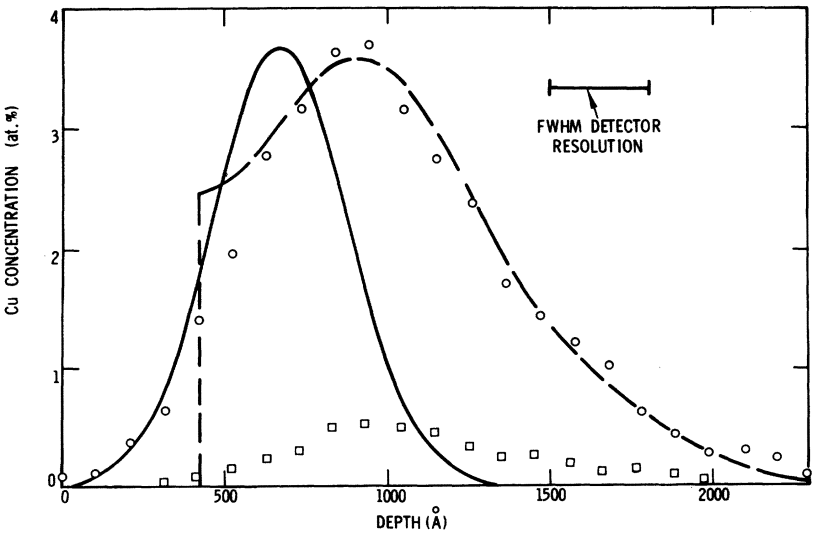

FIG. 2. Depth profiles for Cu implanted into Be at 100 keV. Circles: 4×10^{16} Cu/cm^2. Squares: 7×10^{15} Cu/cm^2. Solid line: prediction of LSS theory, assuming a Gaussian shape. Dashed line: starting profile $C_0(x)$ used in Eq. (3).

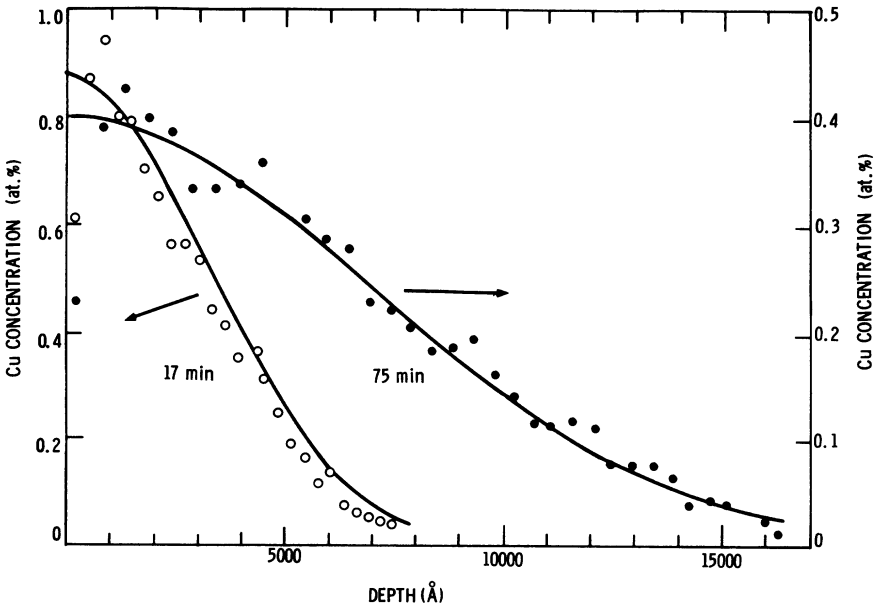

FIG. 3. Depth profile for the higher concentration sample of Fig. 2, following annealing at 595 °C. Open circles: 17 min total anneal. Closed circles: 75 min. The curves are calculated from Eq. (3) using the function shown in Fig. 2 for $C_0(x)$, and adjusting D to agree with the data. Depth is measured from the BeO-Be interface.

Two of the Cu concentration profiles for the sample of Fig. 2, taken during a series of isothermal anneals at 595 °C, are shown in Fig. 3. The solid lines are the calculated profiles using $C_0(x)$ as shown in Fig. 2. The area under the calculated profile was not allowed to change that of $C_0(x)$. Only one parameter, D, was adjusted in each case to produce a best least-squares fit to the data. The area under the experimental profiles is thus seen to be conserved, which confirms that no Cu is being lost from the region of observation. The experimental and theoretical shapes are in good agreement, indicating that no significant trapping of the Cu is present. Both profiles are nearly Gaussian, a necessary condition for the simplified analysis via Eq. (7) where D is calculated from the slope of W^2 vs t. The fitted values of D are 4.4×10^{-13} cm^2/sec for the 17-min anneal and 5.2×10^{-13} cm^2/sec for the 75-min anneal. By comparison, the slope of W^2 vs t gives $D=4.8\times10^{-13}$. Thus the data exhibit a high degree of internal consistency. However, this consistency is maintained only when the Cu has diffused beyond about twice its initial range of 900 Å. The diffusion rate for shorter distances is found to be anomalous.

In Fig. 4 we show a plot of W^2 vs anneal time t for diffusion along the a axis at 420 °C. These particular data, taken at the lowest temperature of the experiment, were selected because they most clearly exhibit the initial behavior of the Cu.

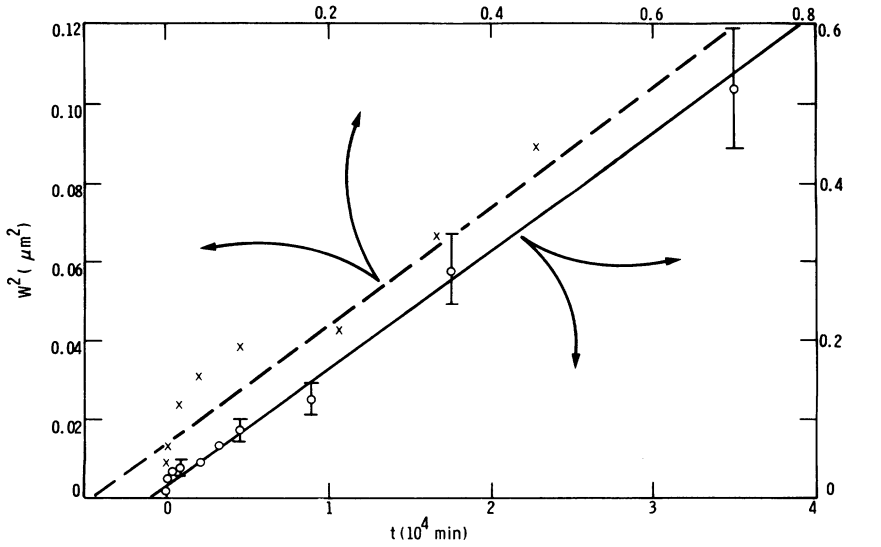

FIG. 4. Plot of W^2 vs t for a Cu implanted a-axis sample at 420 °C. The crosses and dashed line correspond to the same data on an expanded scale. The slope of the straight line yields $D=8.5\times10^{-16}$ cm^2/sec.

The parameter W is seen to increase initially at a relatively high rate to about 2000 Å, to then briefly come to an almost complete stop, and finally to vary as expected from Eq. (7). A detailed analysis using Eq. (3) confirms the anomaly. For example, the fitted value of D at a total anneal time of 412 min is larger by a factor of $\simeq 2$ than that obtained from the slope of the linear region of W^2 vs t. This anomalous behavior for $W \lesssim 2000$ Å was consistently observed for $T \lesssim 500$ °C, but its detailed characterization became more difficult with increasing temperature because of limitations on the accuracy of our measurement at short anneal times. It should be noted here that the diffusion anomalies reported in Ref. 1 for the lower anneal temperatures are consistent with these observations, since the former were found for small values of W. As in Ref. 1, we tentatively suggest that damage introduced during implantation does not completely anneal out at room temperature, and that an associated enhancement of the diffusion occurs during the initial stages of annealing. Fortunately, the linear region of the W^2 vs t plot predicted by Eq. (7) always predominated, and it was from the slope of this region that we calculated D.

B. Vapor-deposited Cu

We have annealed a number of Be samples which had been vapor deposited with Cu to a nominal thickness of either 300 or 3000 Å. Most were isochronally heated: 30-min anneals at 50 °C intervals between 400 and 800 °C. However, two 3000-Å samples were subjected to an isothermal series at 750 °C. Both flowing nitrogen gas and flowing forming gas (10 at.% H_2, 90 at.% N_2) were used, and one of the isothermal series at 750 °C was done under a vacuum of $< 10^{-6}$ Torr. As will be discussed below, in no case were we able to extract a value of D which we felt corresponded to bulk diffusion in the dilute limit. The primary complicating factor was the substantial oxidation, which occurred in all cases, even the vacuum anneal. However, in all of the film data certain qualitative features occurred consistently, and these lead to general conclusions concerning the Cu-Be-O system.

One consistent feature of the film anneal behavior was that, if before the Cu film was oxidized to its full depth, observable interdiffusion of the Be and Cu occurred (typically at $T \gtrsim 500$ °C), then a layer of BeO would form at the surface. This layer would tie up the oxygen from any surface copper oxide layer that had been present and the Cu would be excluded from the newly formed BeO surface layer. Continued heating would cause the BeO layer to grow, and the Cu to diffuse ever deeper into the host with no apparent surface trapping. This phenomenon is illustrated in Fig. 5, which shows a 2-MeV He^+ backscattering spectrum for one of the samples which before annealing had been deposited with 3000 Å of Cu. The spectrum was taken after a full isochronal anneal sequence, ending with 30 min at 800 °C, done under flowing forming gas. It is immediately evident that the leading edge of the diffused Cu profile is displaced from the surface. By contrast, the observed high-energy edges of O and Be indicate that both these elements are present at the surface.

A quantitative analysis of the spectrum in Fig. 5 is readily carried out using the published He energy loss rates S for Be, O, and Cu,[22,27] by assuming that in an alloy these rates are additive (Bragg rule),[28] and by comparing the Cu amplitude with that obtained for a pure Cu reference sample.[29] The nearly flat portion of the Cu spectrum on the right-hand side of the O peak has an amplitude corresponding to 2.3-at.% concentration. This

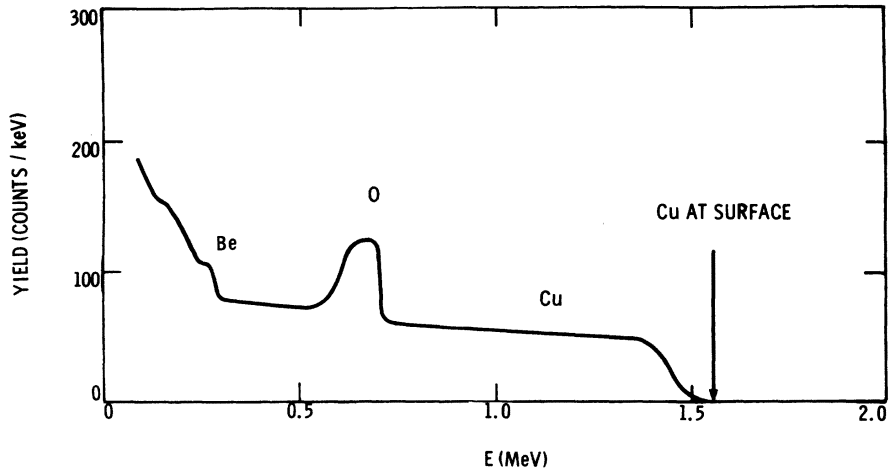

FIG. 5. Energy spectrum of 2-MeV He^+ backscattered from a Be a-axis sample deposited with 3000 Å of Cu, following a series of isochronal anneals ending with 30 min at 800 °C.

corresponds to a region extending from the surface to a depth of 1.7 μm within the sample, over which it is evident that no trapping of the Cu occurs. The step in the Be spectrum is associated with the change from oxide to Be metal, and the amplitude of this step corresponds within experimental error to the composition Be_1O_1. The thickness of the BeO layer, obtained from the width of the O peak, is (1500 ± 200) Å. This may be compared with the distance between the surface of the sample and the onset of the Cu as measured by the half-amplitude point of the Cu profile, which is calculated to be (1300 ± 200) Å. Thus we are led to propose the gettering of the O by the Be and the exclusion of Cu from the oxide layer. This behavior is consistent with that observed for implanted Cu, and is not surprising when one considers the heats of formation of the respective metal oxides. The value for BeO, −144 g-kcal/mole, is much larger than that for CuO, −38, or for Cu_2O, −41.[30] Consequently, the formation of BeO is energetically favored over the Cu oxides.

When oxidation of the Cu film proceeded through the full depth of the film prior to observable interdiffusion with the Be, then the behavior of that film during subsequent anneals was quite different from that described above. In this case a variable but always large fraction of the Cu was trapped at the surface, even up to 800 °C. This occurred consistently for the isochronal anneal sequences of the thinner (300-Å) films, and also for one 3000-Å film when sufficient care was not taken after anneals to cool the sample fully before exposing it to air. However, backscattering spectra in these cases also exhibited some Be at the surface, suggesting lateral nonuniformities. We are not certain of the origin of this behavior, but suggest that it may be due to the breakup of the film during oxidation. This hypothesis is prompted by the fact that oxidation of Cu to either Cu_2O or CuO involves a volume expansion of a factor of $\simeq 1.7$. Such expansion might result in regions of the Cu film not being in contact with the Be substrate. These regions would then remain as an oxide of Cu, while other regions would react with the Be. Under such conditions it is obviously impossible to reliably extract diffusion rates.

In Figs. 6 and 7 we show selected He^+ and proton backscattering spectra from a Cu film sample for an isothermal series of anneals at 750 °C, under flowing dry N_2. Approximate depth scales may be specified by observing that an energy width of 0.1 MeV on the Cu spectrum corresponds to about 2000 Å for He^+ and 20 000 Å for protons. In passing we note the strong enhancement of the proton backscattering yield from Be at 2 MeV—a factor of $\simeq 14$ above that given by the Rutherford cross section. The step in Fig. 7 located just above that part of the spectrum corresponding to elastic scattering from Be may be identified by its high-energy edge, which is consistent with the Be^9 (p, d) nuclear reaction. The thickness of the Cu film before annealing is calculated from the width of the associated peak in Fig. 6 to be 2900 Å. The O peak before annealing is located at an energy corresponding to the O being located at the Be-Cu interface. This oxide was present before the Cu deposition. After 30 min at 750 °C the Cu had diffused into the Be (dashed line in Fig. 6). The high-energy edges of the Be and O spectra show that both these elements are now at the surface. While the oxide peak is not as wide as that in Fig. 5, the exclusion of the Cu from the surface layer of BeO is again evident.

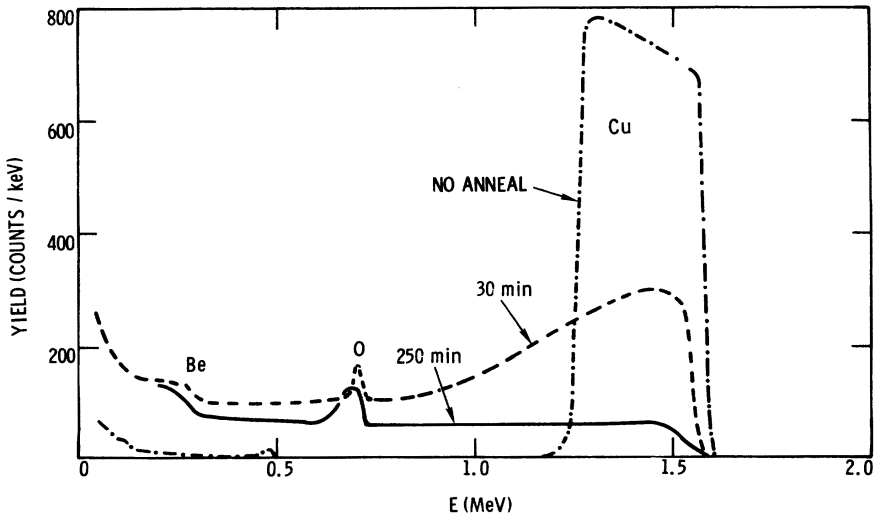

FIG. 6. Energy spectra of 2-MeV He^+ backscattered from a Be c-axis sample deposited with 3000 Å of Cu. Dot-dashed line: no anneal. Dashed line: 30 min total anneal at 750 °C. Solid line: 250 min at 750 °C.

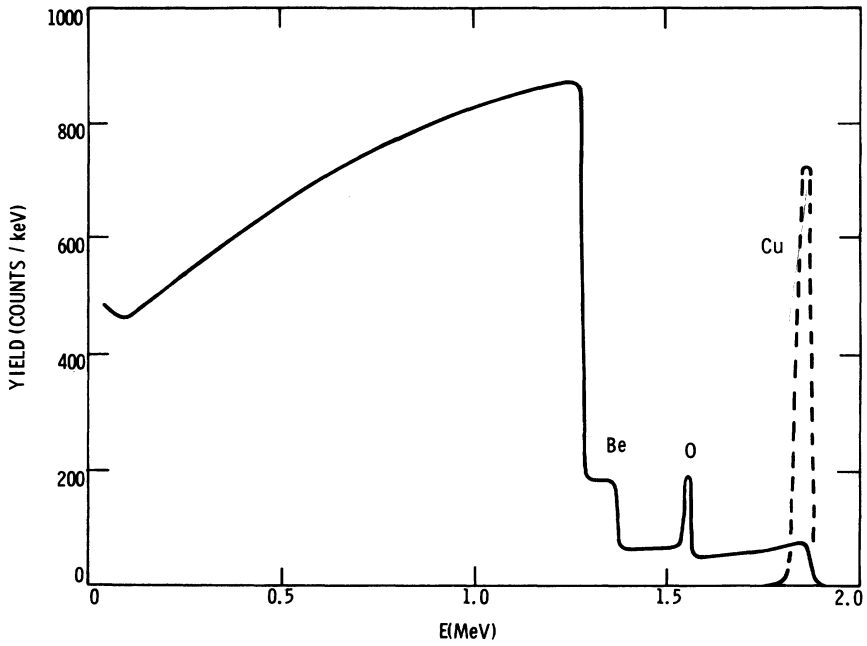

FIG. 7. Energy spectra of 2-MeV protons backscattered from the sample of Fig. 6. Dashed line: no anneal. Solid line: 250 min at 750 °C.

The Cu spectrum in Fig. 6 for the 30-min anneal shows two distinct regions: a tapering peak at the higher energies, followed by a plateau as the energy decreases. Careful observation of this plateau during annealing shows that it initially increases relatively rapidly to the amplitude shown in the figure, then stays nearly constant until the high-energy peak has dropped to the same amplitude. From that point forward the Cu spectrum is almost flat, as seen for the 250-min anneal shown in Figs. 6 and 7, while continuously decreasing in amplitude. This behavior suggests that various Be-Cu intermetallic compounds are formed in the near-surface region at first, but that the Cu concentration in the deeper part of the sample is limited by the solubility of Cu in hcp Be. From the spectra this solubility is calculated to be $(5.5 \pm 1.0)\%$ at 750 °C, which corresponds well to the value of 5.0% taken from the published phase diagram.[31]

In principle, it would seem possible to determine diffusion coefficients from film data such as those shown in Figs. 6 and 7. The total number of Cu atoms per unit area is known from the preanneal spectrum, and if one assumes a Gaussian concentration profile after the Cu concentration has everywhere dropped below the solubility limit, then the parameter W can be deduced from the level of the near-surface plateau. We have attempted this, and within the experimental error, $W^2 \propto t$ as predicted by Eq. (7). However, the resulting D values at 750 °C fell below extrapolations of lower temperature data from the implanted samples, by factors of $\simeq 2$ for the a axis and $\simeq 5$ for the c axis. In view of these large discrepancies, and because sufficient depths could not be probed in these ion backscattering measurements to determine the full concentration profile, we do not think these D values are sufficiently reliable to be used. It may be that once a high concentration of Cu has been present in a region of the sample, that region is no longer single-crystal hcp Be. If so, then the diffusion coefficient would be different near the surface, and greater probing depths than available in these measurements would be required in order to determine D from the profile widths. Much greater diffusion depths are typically used in radiotracer-sectioning techniques to measure high-temperature diffusion.

C. Diffusion rate for dilute Cu in Be

The diffusion coefficient D for dilute Cu in Be, as determined from the implanted samples, is

TABLE I. Diffusion coefficient D for dilute Cu in Be. The experimental uncertainty is ±25% except at 640 °C, where it is ±35%.

	D (cm^2/sec)	
T (°C)	a axis	c axis
420	8.5×10^{-16}	
460		3.1×10^{-15}
521	9.8×10^{-14}	
527		3.6×10^{-14}
595	1.09×10^{-12}	4.8×10^{-13}
640	3.9×10^{-12}	

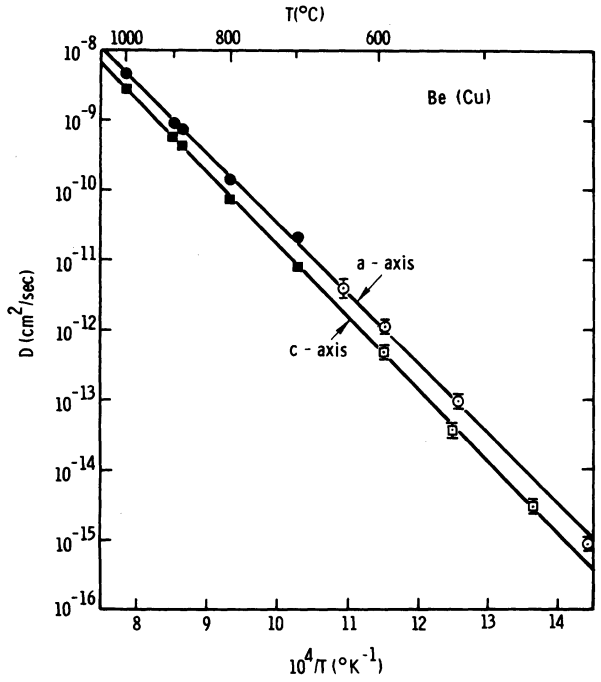

FIG. 8. Temperature dependence of the diffusion coefficient D for dilute Cu and Be. Circles: a axis. Squares: c axis. Open symbols are taken from the present work, the closed symbols from Ref. 2. Straight lines are given by Eqs. (13) and (14).

tabulated in Table I and plotted in Fig. 8. Also given in the figure are the higher-temperature values of Ref. 2. The lines in the figure are given by

$$D_a = (0.416\ \mathrm{cm}^2/\mathrm{sec})\, e^{-23\,230\ ^\circ\mathrm{K}/T} \tag{13}$$

and

$$D_c = (0.381\ \mathrm{cm}^2/\mathrm{sec})\, e^{-23\,870\ ^\circ\mathrm{K}/T}\ , \tag{14}$$

and the corresponding activation energies are (2.00 ± 0.10) eV for the a axis and (2.05 ± 0.10) eV for the c axis. The preexponential factors in these equations are extremely sensitive to the values chosen for the activation energies, and consequently might be in error by as much as a factor of 2. The observed linear variation of $\ln(D)$ with T^{-1} constitutes evidence additional to that presented in Sec. IV A that what we have measured is the bulk diffusion rate. Furthermore, our data are seen to be quite consistent with the higher-temperature values of Ref. 2. The Cu diffusion coefficients are much smaller than those for Be self-diffusion: a factor of $\cong 160$ at 600 °C.[5] However, the anisotropy of diffusion is almost the same: $D_c/D_a = 0.47 \pm 0.10$ for Cu and 0.42 for Be at this temperature.

In order to compare the above data with predictions of the LeClaire model,[4,19] we first determine the jump rates τ_α^{-1} and τ_β^{-1} by applying Eqs. (8) and (9) and setting the correlation factors $f = 1$. The results may be expressed in the form

$$\tau^{-1} = (\tau^{-1})_0\, e^{-Q/k_B T}\ , \tag{15}$$

where $(\tau_\alpha^{-1})_0 = 0.364 \times 10^{15}$ sec^{-1} and $(\tau_\beta^{-1})_0 = 0.395 \times 10^{15}$ sec^{-1}, and the activation energies are $Q_\alpha = (1.98 \pm 0.10)$ eV and $Q_\beta = (2.05 \pm 0.10)$ eV. The corresponding energies for self-diffusion of Be which were reported in Ref. 5 are 1.61 and 1.72 eV, respectively, giving $\Delta Q_\alpha = +0.37$ eV and $\Delta Q_\beta = +0.33$ eV. These experimental values of ΔQ may be compared with the respective theoretical values of +0.80 and +0.90 eV from Sec. IV B. This large discrepancy is well outside the experimental uncertainty, and suggests that a more sophisticated theory is needed.

It is appropriate at this point to compare the above results with those reported for diffusion of dilute Ag in Be.[3] Ag has the same valence as Cu, and hence, within the LeClaire model, should have the same activation energies. However, the activation energies obtained experimentally for D_a and D_c are 1.88 and 1.70 eV, respectively.[32] The former value is intermediate between 1.63 for self-diffusion and 2.00 for Cu, while the latter is very close to the self-diffusion activation energy at 1.71 eV. It is not surprising that Ag behaves quite differently from Cu, in spite of the prediction of a simple electrostatic model of atomic interactions. Nevertheless, it does seem remarkable that the a-axis activation energy changes from that for self-diffusion while the activation energy for the c axis does not. Furthermore, the anisotropy of diffusion for Ag at 656 °C, the lowest temperature for which data were reported in Ref. 3, is $D_c/D_a = 2.24$. This is opposite from the anisotropy for Cu, which is $D_c/D_a = 0.5$ at this temperature. Results such as these would seem to warrant further study of the diffusion of the noble metals in Be.

D. Diffusion during Ne bombardment

We have indicated above that the diffusion of implanted Cu in Be shows some evidence of enhancement for diffusion distances comparable with the ion range. This is believed to be associated with the implantation damage, which increases the vacancy concentration above the thermal equilibrium value. However, a quantitative interpretation is difficult for at least two reasons. First, since the Cu atom comes to rest at the end of a damage track, it does not see a random distribution of vacancies. Second, the damage is introduced at room temperature before annealing, so that damage may accumulate prior to the anneal.

In a preliminary effort to determine the sensitivity of the Cu diffusion rate to radiation damage under better-defined conditions, we have performed

annealing during bombardment by inert-gas ions. A 30-min anneal at 500 °C was carried out on a c-axis sample during bombardment by 2.6×10^{13} Ne/cm^2 sec at 260 keV. The Cu had previously been introduced by implantation at room temperature to a total fluence $\approx 5\times10^{16}$/cm^2 as described in Sec. III. The depth of Cu diffusion during bombardment was less than 3000 Å, which was sufficiently small in comparison to the calculated Ne range of 4900 Å to preclude a significant interaction of the two species. Comparison between Ne-bombarded and unbombarded sections of the sample was made after the anneal. The inert-gas bombardment had no resolvable effect ($\Delta D < 30\%$) on the diffusion rate.

To assess the significance of this negative result it is useful to estimate the rate of production of atomic displacements by the Ne. Brice has calculated the energy deposition into atomic processes in the present experiment[24] using methods described previously,[33] and has found it to be $\simeq 1.3\times10^5$ eV/Ne. As a first approximation we assume the distribution to be uniform over the ion range, 4900 Å. Then the concentration of atomic displacements introduced per atom (dpa) per unit time in this region is given by

$$R = \frac{1}{2}\left(\frac{1.3\times10^5\ \text{eV/Ne}}{4.9\times10^{-5}\ \text{cm}}\right) \times \frac{(2.6\times10^{13}\ \text{Ne/cm}^2\ \text{sec})}{(25\ \text{eV/Be})(1.23\times10^{23}\ \text{Be/cm}^3)} = 0.011\ \text{dpa/sec}\ , \quad (16)$$

where the energy required for one atomic displacement is taken to be about 25 eV. The factor of $\frac{1}{2}$ is due to the requirement that a displaced Be atom have more than twice the displacement energy in order to produce another displacement.[34]

Enhancement of the diffusion rate is a function of the vacancy concentration C_v relative to its value C_{v0} in the absence of irradiation. It therefore depends on the vacancy removal rate as well as the creation rate R. The equilibrium between these processes has been discussed by Dienes and Damask,[35] who point out that the removal may occur via vacancy-interstitial recombination, by diffusion to sinks within the damaged layer, or through diffusion out of the damaged layer. Only the effect of the diffusion out of the damage layer can be estimated with the information presently available. Neglecting the other two mechanisms of removal, one obtains

$$\frac{C_v}{C_{v0}} \simeq \frac{RX^2}{4D_{\text{Be}}} + 1\ , \quad (17)$$

where X is the thickness of the damaged layer and D_{Be} is the Be self-diffusion rate in the absence of irradiation. Under the above irradiation condition,

$$\frac{RX^2}{4D_{\text{Be}}} + 1 \simeq 2.6\ .$$

Since no enhancement was observed, it seems probable that one or both of the other two removal processes must be considered. Experiments at larger values of R are planned to clarify this situation.

V. CONCLUSION

We have measured the diffusion coefficient for dilute Cu in Be between 420 and 640 °C using ion implantation to introduce the Cu and ion backscattering to determine its depth profile. The data are consistent with results obtained by the radioactive tracer method in the range 700–1000 °C, thus tending to confirm the validity of the two experimental techniques. The model of LeClaire for heterovalent impurity diffusion gives poor agreement with the over-all change in activation energies from those of self diffusion. Hopefully, a more realistic theoretical calculation, such as one based on the pseudopotential approach,[36] will become available in the future. Also needed is a theoretical treatment of the anisotropy of the preexponential factor.

Annealing studies of vapor-deposited Cu films on Be have yielded several conclusions concerning the Be-Cu-O system. In general, when Be and Cu are present together gettering of oxygen by Be is observed, accompanied by the formation of a surface layer of BeO from which Cu is excluded. However, full oxidation of a Cu film prior to Be-Cu alloy formation seemed to partially decouple that film from the Be host. This is believed to be due to a breakup of the film because of the volume expansion associated with Cu oxidation. Also, annealing of the Cu films on the Be substrate yielded the solubility limit of Cu in Be. The value of (5.5 ± 1.0) at.% obtained at 750 °C is in good agreement with the published phase diagram.

The effect of radiation damage on the Cu diffusion was studied by annealing at 500 °C under Ne bombardment, with the experimental conditions such that the displacement rate $R \simeq 0.01$ dpa/sec. No evidence of radiation enhancement was observed at this level of damage production.

ACKNOWLEDGMENTS

The authors are indebted to W. Beezhold for the use of the implantation facility and to D. K. Brice for his calculation of the ion ranges and the energy deposition into atomic processes. Helpful conversations with these colleagues and with A. R. Ducharme and J. A. Ellison are acknowledged. Valuable technical assistance was provided by C. T. Fuller, J. Smalley, and R. G. Swier.

*Work was supported by the U. S. Atomic Energy Commission.

[1]S. M. Myers, W. Beezhold, and S. T. Picraux, Proceedings of the Third International Conference on Ion Implantation, Yorktown Heights, New York, 1972 (unpublished).

[2]J. M. Dupouy, J. Mathie, and Y. Adda, *Proceedings of the International Conference on the Metallurgy of Beryllium, Grenoble*, 1965 (Presses Universitaires de France, Paris, 1965), p. 159.

[3]M. C. Naik, J. M. Dupouy, and Y. Adda, Mémoires Scientifiques Rev. Metallurg. 63, 488 (1966).

[4]A. D. LeClaire, Philos. Mag. 7, 141 (1962).

[5]J. M. Dupouy, J. Mathie, and Y. Adda, Mémoires Scientifiques Rev. Metallurg. 63, 481 (1966).

[6]See, for example, J. W. Mayer, I. V. Mitchell, and M. - A. Nicolet, *Proceedings of the Second International Conference on Ion Implantation in Semiconductors*, edited by I. Ruge and J. Graul (Springer-Verlag, Berlin, 1971), p. 274.

[7]R. F. Sippel, Phys. Rev. 115, 1441 (1959).

[8]S. Kawasaki and E. Sakai, J. Nucl. Sci. Tech. 4, 273 (1967).

[9]J. K. Hirvonen, W. H. Weisenberger, J. E. Westmoreland, and R. A. Meussner, Appl. Phys. Lett. 21, 37 (1972).

[10]A. Fontell, E. Arminen, and M. Turunen (unpublished).

[11]J. A. Borders, Thin Solid Films 19, 359 (1973).

[12]G. M. Hood, Philos. Mag. 21, 305 (1970).

[13]G. M. Hood and R. J. Schultz, Philos. Mag. 23, 1479 (1971).

[14]G. M. Hood and R. J. Schultz, Phys. Rev. B 4, 2339 (1971).

[15]S. M. Myers and R. A. Langley, in *Applications of Ion Beams to Metals*, edited by S. T. Picraux, E. P. EerNisse, and F. L. Vook (Plenum, New York, to be published).

[16]S. M. Picraux and G. S. Thomas, in Ref. 15.

[17]See, for example, B. I. Boltaks, *Diffusion in Semiconductors* (Academic, New York, 1963), p. 102.

[18]A review of impurity diffusion has been given by N. L. Peterson, *Solid State Physics*, edited by F. Seitz, D. Turnbull, and H. Ehrenreich (Academic, New York, 1968), Vol. 22, p. 409.

[19]For a detailed discussion of diffusion in the hcp structure, see P. B. Ghate, Phys. Rev. 133, A1167 (1964).

[20]See, for example, N. L. Peterson and S. J. Rothman, Phys. Rev. B 1, 3264 (1970).

[21]See, for example, S. T. Picraux and F. L. Vook, Appl. Phys. Lett. 18, 191 (1971); and J. F. Ziegler and J. E. E. Baglin, J. Appl. Phys. 42, 2031 (1971).

[22]W. K. Chu and D. Powers, Phys. Rev. 187, 478 (1969).

[23]J. Lindhard, M. Scharff, and H. E. Schiott, Kgl. Danske Videnskab. Selskab, Mat. -Fys. Medd. 33, No. 14 (1963).

[24]D. K. Brice (private communication).

[25]O. Almén and G. Bruce, Nucl. Instrum. Methods 11, 257 (1961).

[26]See, for example, the recent work by F. N. Schwettmann, Appl. Phys. Lett. 22, 570 (1973), and references cited therein.

[27]P. D. Bourland, W. K. Chu, and D. Powers, Phys. Rev. B 3, 3625 (1971).

[28]See, for example, P. D. Bourland and D. Powers, Phys. Rev. B 3, 3635 (1971); D. Powers, A. S. Lodhi, W. K. Lin, and H. L. Cox, Thin Solid Films 19, 205 (1973).

[29]A description of the analytical methods may be found in Ref. 21.

[30]See, for example, *Handbook of Chemistry and Physics* (Chemical Rubber Publ. Co., Cleveland, Ohio, 1972).

[31]See, for example, M. Hansen, *Constitution of Binary Alloys*, 2nd ed. (McGraw-Hill, New York, 1958), p. 282.

[32]Note that two different sets of activation energies are listed for Ag in Ref. 3. We have used those given in the abstract because they seem to correspond more closely to the data.

[33]D. K. Brice, Radiat. Effects 6, 77 (1970).

[34]G. H. Kinchin and R. S. Pease, Rep. Prog. Phys. 18, 1 (1955).

[35]G. J. Dienes and A. C. Damask, J. Appl. Phys. 29, 1713 (1958).

[36]See, for example, W. A. Harrison, *Pseudopotentials in the Theory of Metals* (Benjamin, New York, 1966).